

## FAST PROTECTION AGAINST ISLANDING AND UNWANTED TRIPPING OF DISTRIBUTED GENERATION CAUSED BY GROUND FAULTS

Konstantin Pandakov  
NTNU – Norway

konstantin.pandakov@ntnu.no

Hans Kristian Høidalen  
NTNU – Norway

hans.hoidalen@elkraft.ntnu.no

Jorun Irene Marvik  
SINTEF – Norway

jorun.irene.marvik@sintef.no

### ABSTRACT

*Ground faults (GF) in a feeder with interconnected distributed generation (DG) might lead to overvoltages in healthy phases even after feeder disconnection from a substation, obstacles for reclosing schemes, and safety hazards. It requires urgent disconnection of DG to prevent islanding. On the other hand, fast location of GF in compensated networks is a difficult task and finding of the correct fault location is necessary in order to decrease a number of undesirable DG decoupling.*

*The current paper proposes a communication-based scheme preventing islanding forming in a system. The scheme utilizes a new fast and universal indicator revealing fault positions. A locating algorithm is also applied to restrict unwanted disconnection of DG. The method is tested on a model in PSCAD/EMTDC of an actual 22 kV multiterminal grid grounded by a Petersen coil and including DG.*

*The results show that the new indicator can reliably discriminate faults in the system. It has been found that precision of the locator utilizing two-point measurements is not sufficient and might lead to nuisance tripping of the DG. Using of multi-point measurements and the proposed indicator helps to solve this problem for a complex feeder topology. Finally, the same signals can be applied to enhance accuracy of the locator.*

### INTRODUCTION

Proliferation of distributed generation in power systems leads to several complications linked to dependability of the traditional protection schemes. Ground faults bring special issues in compensated and isolated networks. References [1] and [2] show that DG has no impact on performance of ground relays; however, for reliable and safe operation, it is necessary to disconnect interconnected generators as fast as possible. Undervoltage protection, used for this purpose, might lead to unnecessary decoupling of DG in case of faults in adjacent feeders or in downstream locations. On the other hand, relaxing of its settings and having proper fault right through capability can cause unintentional islanding in a system.

[3] describes the state-of-the-art methods on anti-islanding protection. The main purpose of such methods is to detect loss-of-main situation from DG point of view in a network a feeder circuit breaker is open. Taking into

account that the vast majority of faults in distribution networks are single-line-to-ground and they have temporary character, it is advantageous for system reliability to disconnect DG as fast as possible and initiate reclosing procedures. It excludes application of complex schemes with check of synchronization and presence of an island if a fault is permanent.

For this purpose, a communication-assisted scheme [4] can be applied as the most reliable and fast approach. DG obtains measurements from a substation (or several depending on configuration) in order to determine a ground fault location:

- If it is inside of a potential island (a monitoring zone), DG must be decoupled.
- If it is outside, DG can continue operation (the standard undervoltage protection can be blocked).

Nevertheless, locating of ground faults in compensated (in this work, such type of grounding is only considered) distribution networks is a difficult task due to weak fault currents. The traditional approach based on steady-state signals with connection of a parallel resistor [5] is out of interest because such procedure leads to delays, switching transients, increase of fault current, and additional investments (for this reason, signaling methods are not considered here).

On the one hand, elimination of the resistor will accelerate operation, but on the other, it will decrease dependability of the methods based on comparison of residual current directions as it was shown in [6]. Therefore, phase-comparison schemes, for example in [7], can be compromised. Approaches based on variation of current magnitudes, for instance due to alternating of compensation rate presented in [8], might be inadequate in networks with cables or can lose sensitivity in case of high impedance faults. Alternative methods, for example based on calculation of zero sequence admittances [9], require pre-fault information, and settings depend on network configuration. Approaches utilizing low-frequency transients require careful study because they depend on network and fault parameters, whereas high-frequency are difficult to implement in practice due to susceptibility to measuring noise.

Incorrect determination of a fault position might lead to nuisance tripping of DG or, in the worst case, unexpected presence of the source. Thus, a new indicator not depending on network or fault parameters is needed to determine whether fault is in front or behind a ground relay. This paper proposes a simple and universal algorithm utilized in the fast communication-based protection in order to prevent potential islanding

situations in a network or unwanted DG disconnection caused by ground faults, as well as to facilitate reclosing schemes in a feeder with DG. Furthermore, for decreasing of outage time, it is desirable to extract information from the same signals about a probable faulty area. The paper also offers an improved method, presented earlier in [10], on ground fault location estimation demanding less computations and with possibility of precision enhancement.

## DEVELOPMENT OF A NEW INDICATOR

Synchronized two-point measurements at a substation and DG are needed in order to find parameters of an equivalent line, Fig.1, through the following equation:

$$\begin{bmatrix} \frac{Y}{2} + \frac{1}{Z} & -\frac{1}{Z} \\ -\frac{1}{Z} & \frac{Y}{2} + \frac{1}{Z} \end{bmatrix} \begin{bmatrix} V_s \\ V_r \end{bmatrix} = \begin{bmatrix} I_s \\ I_r \end{bmatrix}, \quad (1)$$

where  $Z$  is the series impedance,  $Y$  is the shunt admittance,  $V$  and  $I$  are the voltage and the current at the sending (index  $s$ ) and the receiving ( $r$ ) end. All variables are zero sequence quantities.

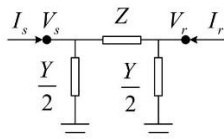


**Figure 1:** Equivalent line.

The next step is to change the real part of the calculated admittance as  $\text{real}(Y)/+j\text{imaginary}(Y)$  because, in most cases, it might be negative during ground faults. Finally, the line is split by the faulty point as shown in Fig.2.

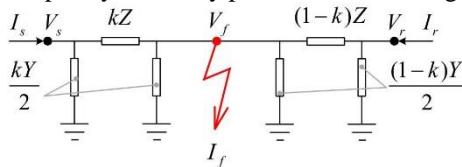


**Figure 2:** Splitting of the equivalent line by the fault.

Hereafter,  $V_f$  is the voltage at the faulty point and  $I_f$  is the fault current. Parameter  $k$  (a relative distance from the sending end) can be determined having the following system of expressions:

$$\begin{cases} V_f = V_s - kZ(I_s - V_s \frac{kY}{2}) \\ V_f = V_r - (1-k)Z(I_r - V_r \frac{(1-k)Y}{2}) \end{cases} \quad (2)$$

It yields the quadratic equation below that is solved for  $k$ .

$$k^2 \frac{ZY}{2} (V_s - V_r) - kZ(I_s + I_r - V_r Y) + V_s - V_r + Z(I_r - V_r \frac{Y}{2}) = 0 \quad (3)$$

The real part of the smallest root is taken as an indicator with the following condition applied in the algorithm:

- $k \approx 0.5$  – the fault is in front of the sending and the receiving relay.
- $k \approx 0$  – the fault is behind one of them.

Such  $k$ -indicator has simple universal settings for the whole system (even if the topology is changed) and immunity to fault origins because equation (3) does not contain  $V_f$  and  $I_f$ . Moreover, any pre-fault information is not needed. This method does not provide information about exact fault location, therefore the algorithm is supplemented by a locator utilizing the same measurements as outlined in the next section.

## DESCRIPTION OF THE ALGORITHM FOR FAULT LOCATION

The same signals obtained from the sending and the receiving end together with pre-fault information about a zero sequence network are used in the locator. It is based on solution of the following matrix equation (in zero sequence quantities):

$$[\mathbf{Z}(k)] \begin{bmatrix} I_s \\ I_r \\ I_1 \\ \dots \\ I_n \\ I_f \end{bmatrix} = \begin{bmatrix} V_s \\ V_r \\ V_1 \\ \dots \\ V_n \\ V_f \end{bmatrix}, \quad (4)$$

In distribution networks there are many load outfeeds between the measuring points as it is illustrated in Fig.3.

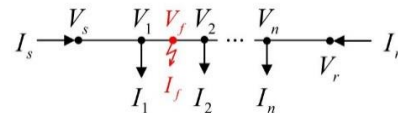


**Figure 3:** Multitapped network.

In (4) they are considered as voltages at load points  $V_1 \dots V_n$  and load currents  $I_1 \dots I_n$ . In compensated systems loads are decoupled from the main trunk by the mean of YD transformers; therefore, for the zero sequence network  $I_1 = \dots = I_n = 0$  is valid.

Equation (4) is nonlinear because zero sequence impedance matrix under fault conditions  $\mathbf{Z}(k)$  is unknown and depends on a fault location. Thus, finding of  $\mathbf{Z}(k)$  provides information about a possible faulty area. It is worth noting that number of measuring points  $N_m$  must be greater or equal to two due to the fact that: the number of the rows  $N$  in (4) is  $N = N_m + N_{ld} + 1$  ( $N_{ld}$  – the number of the load taps), and the amount of the unknowns is  $N_{ld} + 3$  ( $V_1 \dots V_n, V_f, I_f, k$  containing in  $\mathbf{Z}$ ).

The current work proposes the following method for solution:

1. Linearization of  $\mathbf{Z}(k)$ : a fault is assumed to be at a specific position chosen arbitrary, then known  $\mathbf{Z}^*$  can

be formed.

- Vector of currents  $\mathbf{I}$  is determined. In fact, only  $I_f$  is unknown:

$$I_f = \frac{V_m - \mathbf{Z}_{m,1:N-1}^* \cdot \mathbf{I}_{1:N-1}}{\mathbf{Z}_{m,N}^*}, \quad (5)$$

where  $m$  is a row that can be chosen among the rows containing the measured voltages and the currents. Notation  $m,N$  means an element in row  $m$  and column  $N$ . Notation  $1:N-1$  means all elements from 1 to  $N-1$ .

- Calculation of a voltage error. The calculated voltages can be compared with the measured in order to find the most probable fault location. For this purpose, norm of a relative voltage errors is evaluated:

$$\Delta V_{i,l} = \left\| \frac{|\mathbf{V}_{1:N_m} - \mathbf{Z}_{1:N_m,1:N}^* \cdot \mathbf{I}|}{|\mathbf{V}_{1:N_m}|} \right\| \quad (6)$$

where division is elementwise (voltage vector  $\mathbf{V}$  is used), index  $i$  denotes an exact faulty point position on a chosen line  $l$ . Therefore,  $k=i*dk$  with geometrical step  $dk$  and  $i=0:1/dk$ , and  $l=1:N_l$  with the number of lines  $N_l$ .

- The fault position is changed ( $i$  and  $l$  correspondingly) with fixed  $m$ , the matrix of errors is accumulated,  $\Delta \mathbf{V}_{0:1/dk,1:N_l}$ .
- Finding of  $\min(\Delta \mathbf{V})$  gives row  $i^{\min}$  and column  $l^{\min}$  with the minimal element. Values  $k_m^f = i^{\min} * dk$  and  $l_m^f = l^{\min}$  are memorized for fixed  $m$ .
- Additionally, parameter  $\alpha_m$  (for fixed  $m$ ) is calculated as  $\alpha_m = \|\Delta V^{\min_1} \Delta V^{\min_2} \dots \Delta V^{\min_5}\|$ , where  $\Delta V^{\min_{1:5}}$  the first five minimal errors from  $\Delta \mathbf{V}$ .
- Row  $m$  for calculation of  $I_f$  is changed and all steps are repeated. Values of  $k_m^f$ ,  $l_m^f$  and  $\alpha_m$  are accumulated.
- Finally, condition  $\min(\alpha_{1:N_m})$  gives  $m$  that leads to better precision, denoted as  $m-f$ . After that, the most accurate  $k_{m-f}^f$  and  $l_{m-f}^f$  can be chosen.

Steps 6 – 8 differ the proposed approach from the previously developed in [10] and provide higher precision for the locator. Working with an impedance matrix requires fewer computations. Furthermore, in order to speed up calculations, parallel processing is possible (e.g. steps 1 – 6 can be executed simultaneously for different  $m=1:N_m$ ). The performed algorithms have been tested on the model described below.

## TEST CASE NETWORK

Several fault locations have been studied by means of the model of the distribution network illustrated in Fig.4. It is an actual 22 kV grid with DG: a synchronous and an induction generator. Main distribution transformer T1 is grounded through a variable inductor (the value and over compensation rate 3.5 % are provided by the system

operator). The network has overhead transmission lines TL1 – TL22 together with extensive cable sections (specially marked lines TL10\_1, TL10\_3, TL11\_1, TL22\_2). Numerous load points are connected with the main trunks by short cables; detailed modelling of this configuration is bulky, therefore represented as concentrated loads S0 – S19. Protection functions are accomplished by relays R1 – R13.

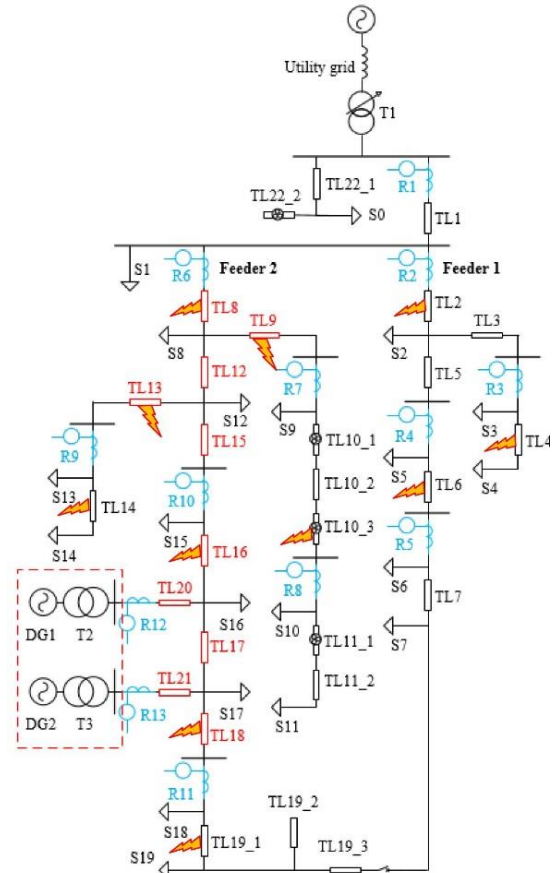


Figure 4: 22 kV distribution network.

The model is built in PSCAD<sup>TM</sup>/EMTDC<sup>TM</sup>: the transmission lines are represented as the PI-equivalent models (electrostatic asymmetry is taken into account), the loads are delta-connected constant impedances (that represents the YD distribution transformers), the utility grid is an ideal voltage source, the transformers and the generators can be found in the standard libraries of the simulation program. All parameters were provided by the system operator and cannot be specified.

Islanding situation will arise in case of faults in the lines marked by red colour in Fig.4 provided that relays R7, R9, R11 successfully clear the downstream faults.

## RESULTS AND DISCUSSIONS

Fig.5 shows dynamic behaviour of the  $k$ -indicator for the faults (inception time is 4.45 s) in Fig.4. In addition to the lines specified above, a fault was applied for different

phases (to handle network asymmetry) and fault resistances – 10 Ohm and 3 kOhm. Relays R6 and R13 are used to identify the equivalent line.

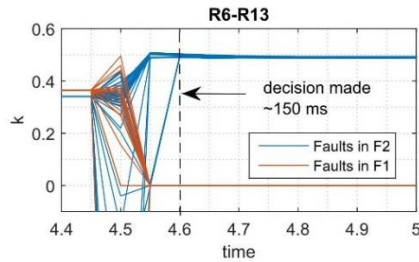


**Figure 5:** Dynamic performance of the  $k$ -indicator.

As it is possible to see, the faults in Feeder 1 are effectively discriminated regardless of fault origins. Moreover, decision is made during the first few hundreds milliseconds (the transient period) that provides possibility for fast operation.

After the correct feeder selection, the faults in lines TL10\_3, TL14, TL19\_1 must be separated from the red-marked in Feeder 2 (Fig.4) in order to prevent nuisance tripping. For this purpose, the fault locator is used. Fig.6 shows the dynamic performance of the locator for the fault in line TL8. Here, post-fault processing of the recorded measurements is applied, step  $dk = 0.01$  is used.

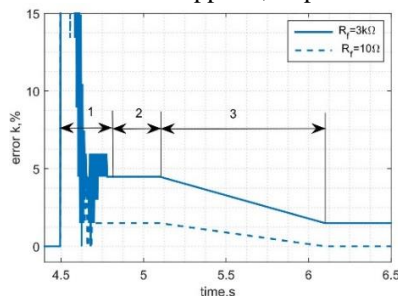


**Figure 6:** Dynamic performance of the fault locator.

In Fig.6, period 1 represents the transient period, and 2 – the steady-state; as it is possible to notice, stable solution for error of  $k_{m-f}^f$  (the line is determined correctly), is achieved in the second period. It is also seen that the low-ohmic fault (higher fault current) leads to the better accuracy. Therefore, a parallel resistor or decrease of the Petersen coil inductance (period 3 reflects gradual process as an example) can be applied: it improves the precision of the locator.

Fig.7a illustrates the calculated results for the faults in phase A with resistance 3 kOhm in the locations mapped on the one-line diagram of Feeder 2. It can be seen that the maximal errors ( $\Delta_{1,2,3}$ ) belong to lines TL10\_3, TL14, TL19\_1 that are the side branches from the main path between relays R6 and R13; in contrast, the more precise results are achieved for lines TL8, TL16. Errors  $\Delta_{1,2,3}$  lead to nuisance tripping of the DG.

Fig.7b demonstrates that the several possible (calculated on the basis of the first five minimal voltage errors  $\Delta V_{1:5}^{\min}$ ) locations for one fault, for example in line TL10\_3, can identify that it is in the side branch. Nevertheless, accuracy required for reliable prevention of nuisance tripping of the DG is still poor even for larger overcompensation.

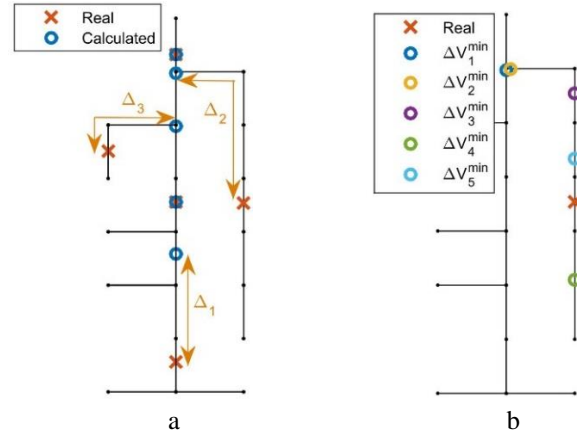


**Figure 7:** Fault location for (a) two-point measurements, (b) line TL10\_3.

#### Algorithm for four-point measurements

In order to avoid unintentional decoupling of DG because of locator error, measurements of relays R6, R7, R9, R11 must be involved. Hence, the  $k$ -indicator can be used to discard the lines downstream of these relays. Fig.8 illustrates this method for the faults in the system for all three phases in each line and two fault resistances – 10 Ohm and 3 kOhm (hence, six cases for each line).

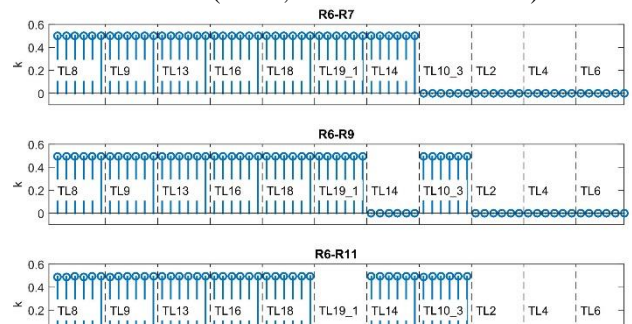


**Figure 8:** The  $k$ -indicator for four-point measurements.

Applying three pairs of relays (R6 – R7, R6 – R9 and R6 – R11), it is possible to construct the equivalent lines and find  $k$  for each pair. It is seen that relays R6 and R7 eliminate ( $k \approx 0$ ) the faulty lines in Feeder 1 and in front of relay R7 (polarity is towards the substation). Analogously, relays R6 and R9 discriminate line TL14 and Feeder 1; relays R6 and R11 – Feeder 1 and TL19\_1.

Applying AND logic between these three pairs, the final decision leave lines TL8, TL9, TL13, TL16, TL18 with  $k \approx 0.5$ . All these lines belong to the area of the potential island; therefore, the DG can be disconnected in a fast



manner. Conversely, if  $k \approx 0$ , the DG continues operation with the grid with respect to its fault ride through capability. Numerous simulations with various network and fault parameters show high reliability of such approach.

Fig.9 illustrates performance of the locator for the faults inside the potential zone: all corresponding lines are correctly identified, and error of  $k$  depends on fault resistance and compensation rate (inductance  $L_1$  is greater than  $L_2$  in the plot).

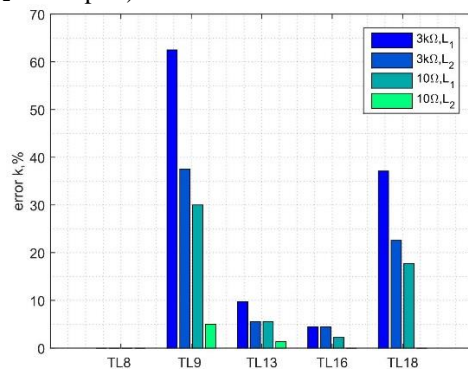


**Figure 9:** Fault location error for four-point measurements.

It is noticeable that the error is small or around zero for the long lines (e.g. TL8, ~15 km) and significant for the short (e.g. TL9, ~500 m).

## CONCLUSION

This work has demonstrated the performance of the proposed  $k$ -indicator for ground fault position identification. It has the following advantages: simple settings coming to logical 1 or 0 (less information in data packages) and not depending on (variable) system configurations, immunity to fault parameters (locations, impedances), fast decisions during few hundreds milliseconds, no need in prefault information.

The improved fault locator based on the zero sequence network demonstrates sufficient usability for the multitapped distribution network. Accuracy can be enhanced by decreasing of a Petersen coil inductance at the substation or using more measurements and the smaller network size.

Application of the proposed algorithm in the real system will benefit as follows:

- Avoiding of unnecessary tripping of the DG caused by ground faults.
- Fast identification of potential islanding situation in case of ground faults in the network followed by disconnection of the DG and initiation of reclosing procedures.
- Accurate ground fault location that improves reliability of power supply.

It is worth mentioning that the basic indicator for ground fault identification and initialization of the performed algorithms can be zero sequence voltage. The further work requires studying of difficulties arising with presence of intermittent faults in cables (unstable signals).

## REFERENCES

- [1] L.K. Kumpulainen, K.T. Kauhaniemi, 2005, "Aspects of the effects of distributed generation in single-line-to-earth faults", *International Conference on Future Power Systems*, 5
- [2] K. Mäki, S. Repo, P. Järventausta, 2007, "Impacts of Distributed Generation on Earth Fault Protection in Distribution Systems with Isolated Neutral", *19<sup>th</sup> International Conference on Electricity Distribution, CIRED*, 4
- [3] S.C. Paiva, H.S. Sanca, F.B. Costa, B.A. Souza, 2014, "Reviewing of anti-islanding protection", *11<sup>th</sup> IEEE/IAS International Conference on Industry Applications, INDUSCON*, 1–8
- [4] E.O. Schweitzer, D. Finney, M.V. Mynam, 2012, "Communications-assisted schemes for distributed generation protection", *IEEE PES Transmission and Distribution Conference and Exposition (T&D)*, 1–8
- [5] I.G. Kulis, A. Marusic, S. Zutobradic, 2004, "Insufficiency of watt-metric protection in resonant grounded networks", *Eighth IEE International Conference on Developments in Power System Protection, DPSP 2004*, vol.2, 486–489
- [6] H. Ji, Y. Yang, H. Lian, S. Cong, 2006, "Effect on Earth Fault Detection Based on Energy Function Caused by Imbalance of Three-Phase Earth Capacitance in Resonant Grounded System", *International Conference on Power System Technology*, 1–5
- [7] D. Jiao, L. Yuping, Z. Guofang, L. Xia, 2009, "An asymmetrical fault location method based on communication system in distribution network with DGs", *IEEE/PES Power Systems Conference and Exposition (PSCE)*, 1–5
- [8] M. Lehtonen, O. Siirto, M. F. Abdel-Fattah, 2014, "Simple fault path indication techniques for earth faults", *Electric Power Quality and Supply Reliability Conference (PQ 2014)*, 371–378
- [9] A. Wahlroos, J. Altonen, 2009, "Performance of novel neutral admittance criterion in MV-feeder earth-fault protection", *20<sup>th</sup> International Conference and Exhibition on Electricity Distribution-Part 1, CIRE*, 1–8
- [10] S. M. Brahma, 2011, "Fault Location in Power Distribution System with Penetration of Distributed Generation", *IEEE Transactions on Power Delivery*, vol. 26, issue 3, 1545–1553